Volume 27
Number 41
7 November 2025
Pages 21853–22290

PCCP

Physical Chemistry Chemical Physics

rsc.li/pccp

25 YEARS ANNIVERSARY

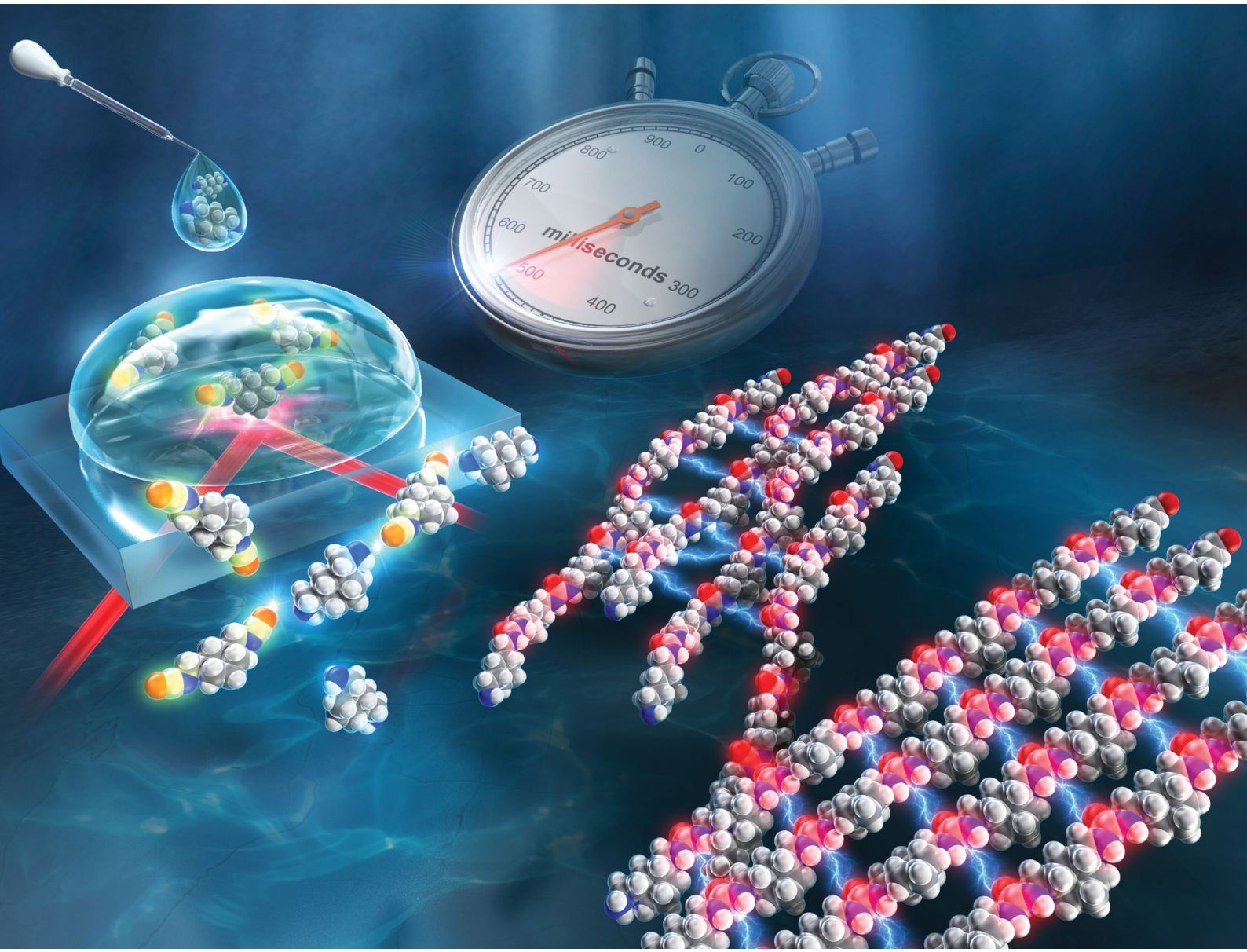

ISSN 1463-9076

ROYAL SOCIETY OF CHEMISTRY

PAPER

Yasuko Koshiba, Kenji Ishida *et al.*

In situ observation of polyurea formation by rapid-scan time-resolved infrared spectroscopy

PCCP Owner Societies

PCCP

ROYAL SOCIETY OF CHEMISTRY

PAPER

View Article Online
View Journal | View Issue

Cite this: *Phys. Chem. Chem. Phys.*, 2025, **27**, 21871

In situ observation of polyurea formation by rapid-scan time-resolved infrared spectroscopy

Yasuko Koshiba, *[ab] Satoshi Atsumi,[a] Tatsuya Fukushima, [ab] Shohei Horike [abc] and Kenji Ishida *[abd]

Received 2nd July 2025,
Accepted 4th September 2025

DOI: 10.1039/d5cp02518d

rsc.li/pccp

Polyurea and its derivatives exhibit excellent physical and chemical properties originating from intermolecular hydrogen bonding. Consequently, they have been used as coating materials that are resistant to heat, water, and chemicals, and in recent years, as materials for 3D printers. Their properties depend on their formation and hydrogen bonding mechanisms; however, these processes are very fast, making them challenging to study experimentally. In this study, polyurea formation *via* the polyaddition reaction of a diamine and diisocyanate was investigated *in situ* by fast time-resolved Fourier-transform infrared-attenuated total reflectance (FTIR-ATR) spectroscopy. This method enabled the analysis of the polyaddition reaction within 1 s and observation of intermolecular hydrogen bond formation. We observed the polyurea formation of different aliphatic and alicyclic monomers by recording the FTIR-ATR spectra every ~0.07 s and analyzed the reaction kinetics. In the case of aliphatic monomers, strong hydrogen bonds were formed in the initial stage of polyurea formation, whereas in the case of alicyclic monomers, weak hydrogen bonds were initially formed, which strengthened as the reaction proceeded. These findings elucidate the role of monomer structure in the formation and hydrogen bonding state of polyurea and demonstrate the effectiveness of time-resolved FTIR-ATR spectroscopy as a technique for observing very fast reactions and intermolecular interactions.

Introduction

Polyurea, the general term used to describe polymeric materials containing urea groups, is formed by the polyaddition reaction of diamine and diisocyanate monomers. It exhibits excellent heat resistance, durability, and chemical resistance owing to strong intermolecular hydrogen bonding.[1–4] The mechanical properties of polyurea produced by reactions between various diisocyanates and diamines have been investigated extensively.[2,5–12] In addition, polyurea exhibits a large electric dipole (4.9 D) derived from the urea group and a high dielectric constant, making it suitable for use in electronic devices and film capacitors.[13–15] It is also widely used as a durable coating material owing to significant advantages, such as fast solvent-free reactions and the ability to tailor its structure and properties by using different monomers.[16–20]

In recent years, polyurea has been investigated as a material for 3D printing.[21,22] 3D printing techniques include fused deposition modeling, light-based resin curing, and curing through the mixing of two or more reactive inks. Polyurea used for 3D printing is formed by mixing and curing diamine and diisocyanate components, making it important to control the polyaddition reaction. To achieve this, observation and analysis of the reaction process are necessary. However, because the polyaddition of a diamine monomer to a diisocyanate monomer is a rapid reaction, few studies have examined the kinetics of polyurea formation in detail. Despite its difficulty, analysis of reaction kinetics is useful in the development of 3D printer materials that require rapid curing. Previously, polyurea formation was analyzed by modifying the monomer structure to slow the reaction. Under conditions of reduced polyurea reactivity, Song and Liu monitored polyurea formation by Fourier-transform infrared (FTIR) spectroscopy on the scale of tens of seconds and analyzed the reaction kinetics.[23] Other polyurethane or poly(urea–urethane) formation reactions have also been examined by FTIR spectroscopy augmented with attenuated total reflectance (ATR) over several tens of minutes,[24,25] demonstrating the usefulness of this method for reaction analysis. However, few reactions have been observed on the seconds timescale.

On the other hand, the formation of intermolecular hydrogen bonds in polyurea is crucial to its excellent mechanical and

[a] *Department of Chemical Science and Engineering, Graduate School of Engineering, Kobe University, 1-1 Rokkodai-cho, Nada-ku, Kobe 657-8501, Japan. E-mail: koshiba@kobe-u.ac.jp, ishida.kenji.383@m.kyushu-u.ac.jp*
[b] *Research Center for Membrane and Film Technology, Kobe University, 1-1 Rokkodai-cho, Nada-ku, Kobe 657-8501, Japan*
[c] *Center for Environmental Management, Kobe University, 1-1 Rokkodai-cho, Nada-ku, Kobe 657-8501, Japan*
[d] *Department of Quantum Physics and Nuclear Engineering, Graduate School of Engineering, Kyushu University, 744 Motooka Nishi-ku, Fukuoka 819-0395, Japan*

chemical properties and has therefore attracted significant attention. Numerous studies have ascribed the hydrogen bonding state of polyurea to its formation conditions, molecular structure, and temperature changes.[2,3,14,26–31]

In this study, we aimed to observe ultrafast polyurea formation *in situ* by rapid-scan time-resolved FTIR spectroscopy.[32,33] To obtain a fundamental understanding of this ultrafast reaction, diamine and diisocyanate monomers with simple, basic aliphatic or alicyclic structures were employed. The ultrafast formation of polyurea was captured in real time, preserving its intrinsic reaction rate. FTIR-ATR spectra obtained over a short observation time of approximately 1 s were used to analyze the reaction kinetics. To clarify the polyurea formation process and the associated intermolecular hydrogen bonding, we conducted a detailed analysis of spectral changes, focusing on the shift in the absorption peak of the urea group. Reaction analysis of the extremely rapid polyurea formation reaction revealed that the hydrogen bond formation process during polymerization varies depending on the monomer structure.

Results and discussion

Polyaddition reaction of hexamethylene diamine (HDA) and hexamethylene diisocyanate (HDI)

Fig. 1a–d shows the chemical structures of the aliphatic diamine HDA, aliphatic diisocyanate HDI, alicyclic diamine H6XDA, and alicyclic diisocyanate H6XDI, respectively. The experimental setup is shown in Fig. 2. FTIR-ATR spectra were acquired at an interval of approximately 70 ms.

Fig. 3 shows the ATR spectra of a 1.0 M HDI/dimethyl sulfoxide (DMSO) solution, 1.0 M HDA/DMSO solution, reaction products mixed with HDA/DMSO and HDI/DMSO, and DMSO. The absorption spectrum of HDI/DMSO exhibited the absorption peaks of DMSO and a strong peak assigned to the antisymmetric N═C═O stretching vibration [ν(N═C═O)] of the diisocyanate monomer at 2260 cm^{-1}.[23,24] On the other hand, peaks related to the N–H stretching vibration [ν(N–H)] at 3325 cm^{-1}, C═O stretching vibration [ν(C═O)] at 1616 cm^{-1}, and N–H bending vibration [δ(N–H)] at 1581 cm^{-1} of the urea group appeared in the spectrum of the product when HDA/DMSO was dropped onto HDI/DMSO.[3,14,23,24,34] These results suggest that polyurea was formed when HDA/DMSO was added to HDI/DMSO.

FTIR-ATR spectra were acquired before and after the addition of HDA/DMSO. Fig. 4a shows the ATR spectra recorded from immediately before the addition of HDA/DMSO (set as 0 s)

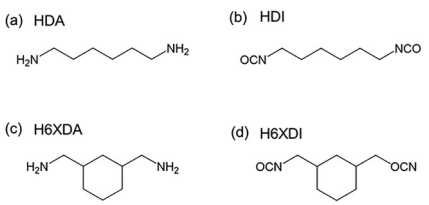

Fig. 1 Chemical structures of (a) hexamethylenediamine (HDA), (b) hexamethylene diisocyanate (HDI), (c) 1,3-bis(aminomethyl)cyclohexane (H6XDA), and (d) 1,3-bis(isocyanatomethyl)cyclohexane (H6XDI).

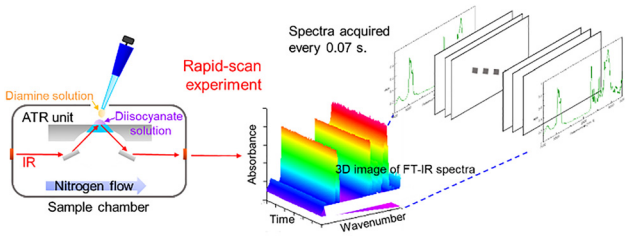

Fig. 2 Schematic of the experimental setup for rapid-scan time-resolved FTIR-ATR spectroscopy.

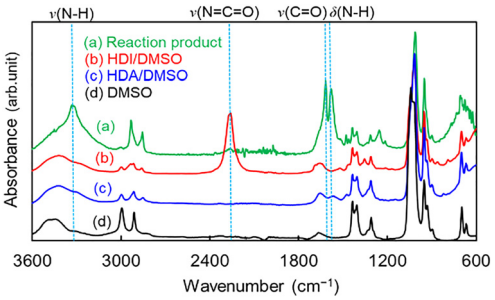

Fig. 3 FTIR-ATR spectra of (a) the product formed by the polyaddition reaction of hexamethylenediamine (HDA)/dimethyl sulfoxide (DMSO) with hexamethylene diisocyanate (HDI)/DMSO, (b) HDI/DMSO, (c) HAD/DMSO, and (d) DMSO.

to 200 s. The initial ATR spectrum showed a strong ν(N═C═O) peak corresponding to HDI at 2265 cm^{-1} and a weak broad peak assigned to DMSO at approximately 1650 cm^{-1}. The intensity of the ν(N═C═O) peak began to decrease 1 s after the addition of HDA/DMSO and disappeared after 10 s. On the other hand, the ν(C═O) and δ(N–H) absorption peaks of the urea group were initially absent in the HDI/DMSO spectrum but appeared 1.0 s after adding HDA/DMSO. Their absorption intensities changed slightly during the 10–200 s period. Therefore, we focused on the period between the addition of HDA/DMSO (0 s) and 1.33 s (during which the ATR spectrum changed significantly) and monitored the ATR spectra every 0.07 s.

The ATR spectra recorded from 0 to 1.33 s are shown in Fig. 4b. The intensity of the absorption peak at 2265 cm^{-1} ascribed to ν(N═C═O) decreased after the addition of HDA/DMSO, along with the simultaneous appearance of the absorption peaks for ν(C═O) and δ(N–H) at 1617 and 1581 cm^{-1}, respectively, which are ascribed to the urea group. The intensities of these two peaks strengthened over time. The polyaddition reaction between a diisocyanate and diamine is generally considered to be extremely rapid. In this experiment, most of the reaction appeared to occur within 1 s from when the

HDA/DMSO solution was dropped onto the HDI/DMSO solution on the ATR prism. The reduction in the number of isocyanate groups and formation of urea moieties within 1 s are due to the polyaddition reaction between HDI and HDA, as evidenced by the changes in the relative peak intensities in the

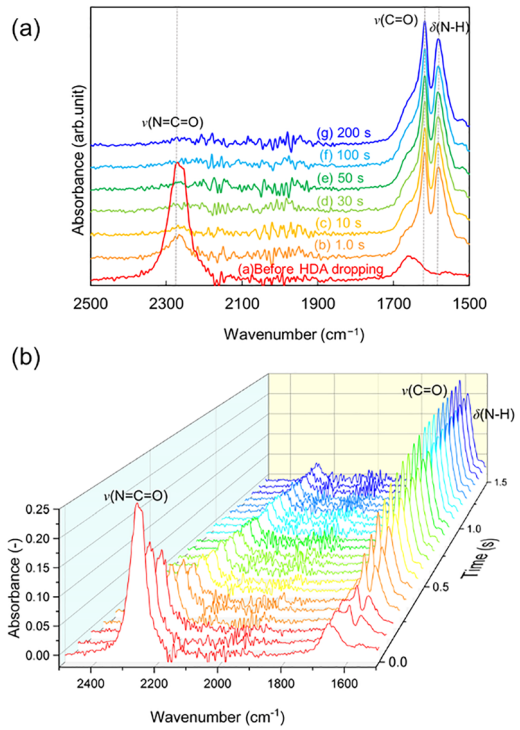

Fig. 4 FTIR-ATR spectra acquired during the polyaddition reaction of hexamethylenediamine (HDA)/dimethyl sulfoxide (DMSO) and hexamethylene diisocyanate (HDI)/DMSO. (a) 0–200 s and (b) 0–1.33 s (0 s corresponds to the point immediately before HDA/DMSO was dropped onto HDI/DMSO).

FTIR-ATR spectra; hence, this technique is effective for observing very fast reactions.

Kinetics of the polyaddition reaction of a diamine and diisocyanate

Rapid-scan time-resolved FTIR spectroscopy was also performed on the polyaddition reaction of 1.0 M H6XDA/DMSO and 1.0 M H6XDI/DMSO using the same method described above. The FTIR-ATR spectra showed absorption peaks related to the ν(N═C═O) mode of the diisocyanate (HDI: 2265 cm^{-1}, H6XDI: 2257 cm^{-1}) and δ(N–H) mode of the urea group (HDI + HDA: 1581 cm^{-1}, H6XDI + H6XDA: 1555 cm^{-1}). The absorbance values of these peaks are plotted as a function of time in Fig. 5a and b from the point at which the diamine solution was dropped onto the diisocyanate solution. The absorbance values were the maximum peak heights for following analysis.

The absorbance of the ν(N═C═O) peak (2265 cm^{-1}) decreased sharply within 1 s after adding HDA/DMSO (Fig. 5a), while that of the δ(N–H) peak (1581 cm^{-1}) increased sharply within the same period. This indicates that polyurea (which contains urea groups) was formed by the polyaddition reaction of the diisocyanate and diamine. In a similar manner, the absorbance of the ν(N═C═O) peak (2257 cm^{-1}) sharply decreased while that of the δ(N–H) peak increased when H6XDI/DMSO reacted with H6XDA/DMSO. We analyzed the reaction kinetics based on the absorbance changes in the initial 1 s of the reaction.

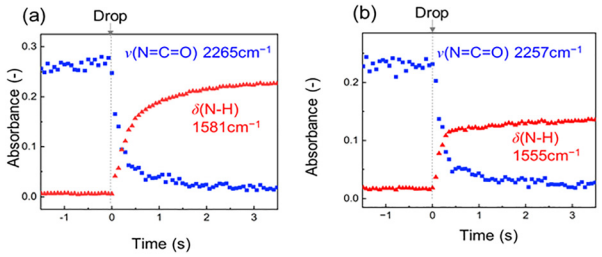

Fig. 5 Absorbance values of the ν(N═C═O) peak related to the diisocyanate and δ(N–H) peak related to polyurea as a function of time during the polyaddition reactions (a) between hexamethylenediamine/dimethyl sulfoxide (DMSO) and hexamethylene diisocyanate/DMSO and (b) between 1,3-bis(aminomethyl)cyclohexane/DMSO and 1,3-bis(isocyanatomethyl)cyclohexane/DMSO.

The polyaddition of a diamine to a diisocyanate is shown in Scheme 1, and the corresponding kinetics equation can be written as

$$\frac{\mathrm{d[polyurea]}}{\mathrm{d}t} = k[\mathrm{diamine}]^{n_1}[\mathrm{diisocyanate}]^{n_2}, \quad (1)$$

where n_1 and n_2 are the reaction orders, t is the reaction time, and k is the reaction rate constant.

We focused on the rate of decrease in the diisocyanate concentration as polyurea formation proceeds when the diamine and diisocyanate solutions are mixed.

$$-\frac{\mathrm{d[diisocyanate]}}{\mathrm{d}t} = k[\mathrm{diamine}]^{n_1}[\mathrm{diisocyanate}]^{n_2}, \quad (2)$$

Eqn (2) can be expressed in terms of the concentrations of the functional groups involved in the formation of the urea group as follows:

$$-\frac{\mathrm{d}c_{\mathrm{NCO}}}{\mathrm{d}t} = k \cdot {c_{\mathrm{NH_2}}}^{n_1} \cdot {c_{\mathrm{NCO}}}^{n_2}, \quad (3)$$

where c_{NCO} and $c_{\mathrm{NH_2}}$ are the concentrations of the –NCO and –NH_2 functional groups, respectively. Because the diamine and diisocyanate concentrations were initially equal in this experiment and the reaction follows a 1 : 1 stoichiometry, eqn (3) can be written as

$$-\frac{\mathrm{d}c_{\mathrm{NCO}}}{\mathrm{d}t} = k \cdot {c_{\mathrm{NCO}}}^{(n_1+n_2)}, \quad (4)$$

where $n = (n_1 + n_2)$ is the reaction order.

Using the Beer–Lambert law, the concentration of the –NCO functional group was calculated from the absorbance of the ν(N═C═O) peak. The ATR spectra of the DMSO solutions of 0.2–1.0 M HDI and H6XDI were acquired, and the absorbance of the ν(N═C═O) peak was plotted against the concentration. The molar absorption coefficient was calculated from the slope

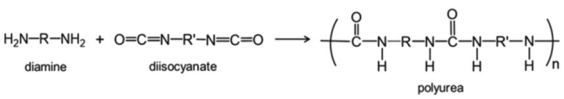

Scheme 1 Polyurea formation *via* the polyaddition of a diamine to a diisocyanate.

of this plot (Fig. S1) and used to determine the concentration of the –NCO functional group. The IR penetration depth of the ATR prism was used as the optical path length (eqn (S1)).[25]

Polyurea and polyurethane are formed through a second-order reaction.[23–25] To confirm the validity of the second-order reaction model used in this study, we applied the half-life method to calculate the reaction order n using concentrations of 0.5 and 1.0 M for the diamine and diisocyanate solutions, respectively (see Section S2). The calculated results confirm that the reaction is second order; consequently, eqn (4) can be written as eqn (5) and integrated to obtain eqn (6):

$$-\frac{dc_{NCO}}{dt} = k \cdot {c_{NCO}}^2, \quad (5)$$

$$\frac{1}{c_{NCO}} = \frac{1}{c_{NCO_0}} + kt, \quad (6)$$

where c_{NCO_0} is the initial concentration of the diisocyanate. Eqn (6) was used to calculate the reaction rate constant k from the slope of the relationship between $1/c_{NCO}$ and the reaction time t.

Fig. 6 shows the variation of $1/c_{NCO}$ with t during the reactions between HDA/DMSO and HDI/DMSO and between H6XDA/DMSO and H6XDI/DMSO. The time at which the diamine solution was dropped onto the diisocyanate solution was set to 0 s, and k values were obtained from the plotted curves by linear regression analysis.

The k value for the polyaddition reaction of HDI/DMSO and HAD/DMSO was 7.75 L mol^{-1} s^{-1} while that for the polyaddition reaction of H6XDI/DMSO and H6XDA/DMSO was 8.21 L mol^{-1} s^{-1}. Thus, in our study, the polyaddition reaction of alicyclic monomers was faster than that of aliphatic monomers in the initial stage. Rapid-scan time-resolved FTIR-ATR spectroscopy facilitated the analysis of the initial stage (first second) of the polyaddition reaction of a diisocyanate and diamine.

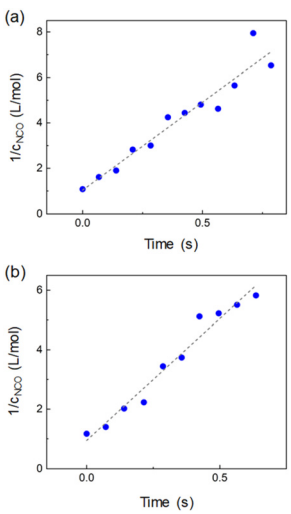

Fig. 6 Reciprocal of the isocyanate concentration (c_{NCO}) as a function of time for the polyaddition reactions (a) between hexamethylenediamine/dimethyl sulfoxide (DMSO) and hexamethylene diisocyanate/DMSO and (b) between 1,3-bis(aminomethyl)cyclohexane/DMSO and 1,3-bis(isocyanatomethyl)cyclohexane/DMSO.

Changes in hydrogen bonding during the polyaddition reaction

The NH group of a urea moiety forms an intermolecular hydrogen bond with the C=O group of another urea moiety, and the positions of the ν(C=O) and δ(N–H) FTIR peaks (derived from the urea group) change according to the hydrogen bonding state.[3,27–30] In general, the ν(C=O) peak shifts to a lower wavenumber, whereas the δ(N–H) peak shifts to a higher wavenumber when hydrogen bonds are formed.[3,27–30] We analyzed the formation of polyurea and intermolecular hydrogen bonding by observing the changes in the positions of these peaks during the polyaddition reaction. The FTIR-ATR spectra for the reactions between 1.0 M HDI/DMSO and 1.0 M HDA/DMSO and between 1.0 M H6XDI/DMSO and 1.0 M H6XDA/DMSO over the first ~100 s after dropping the respective diamine solutions onto the diisocyanate solutions are shown in Fig. 7a and b, respectively.

The spectrum acquired 0.07 s after dropping HDA/DMSO onto HDI/DMSO (Fig. 7a) showed a weak ν(C=O) absorption peak at 1617 cm^{-1}. The intensity of this peak was significantly higher 1 s later and increased slightly as the time further increased to 100 s. However, the position of the ν(C=O) peak did not change over this period (Fig. 7c). In a similar manner, the absorbance of the δ(N–H) peak at 1580 cm^{-1} increased rapidly after adding HDA/DMSO but only increased slightly thereafter (Fig. 7a). The position of this peak also did not change, similar to that of the ν(C=O) peak.

Fig. 7b shows the appearance of a broad ν(C=O) absorption peak at 1666 cm^{-1} 0.07 s after dropping H6XDA/DMSO onto H6XDI/DMSO, and its intensity increased with increasing time (up to 0.49 s). Fig. 7d shows the evolution of the ν(C=O) peak position with time during the reaction. The peak shifted from 1666 cm^{-1} at the initial stage of polyurea formation to ~1656 cm^{-1} after 1 s and then to 1640 cm^{-1} after 10 s. On the other hand, the δ(N–H) absorption peak appeared at 1555 cm^{-1} from 0 to 0.49 s, then shifted to a higher wavenumber (1563 cm^{-1}) at 100 s (Fig. 7b).

The urea group can form three different states of intermolecular hydrogen bonding—ordered, disordered, and free—as indicated by the different ν(C=O) peak positions (*i.e.*, 1630–1645, 1650–1665, and 1685–1710 cm^{-1}, respectively).[2,3,14,27–29] Changes in the intermolecular hydrogen bonding state shift the ν(C=O) peak position by 30–60 cm^{-1}, which is larger than the difference associated with changes in the chemical structure (less than 15 cm^{-1}).[2,14] The ν(C=O) peak was observed at 1617 cm^{-1} from the point at which HAD/DMSO was added to the end of the reaction of the aliphatic monomers (*i.e.*, HDI and HDA). This peak position is approximately 10 cm^{-1} lower than that reported for ordered hydrogen bonding,[2,3,14,27–29] which indicates that the polyurea synthesized from HAD and HDI mainly formed ordered hydrogen bonds. The ν(C=O) peak position did not change during the reaction, which implies that the ordered hydrogen bonds formed in the initial stage were maintained. In contrast, the ν(C=O) peak was observed at

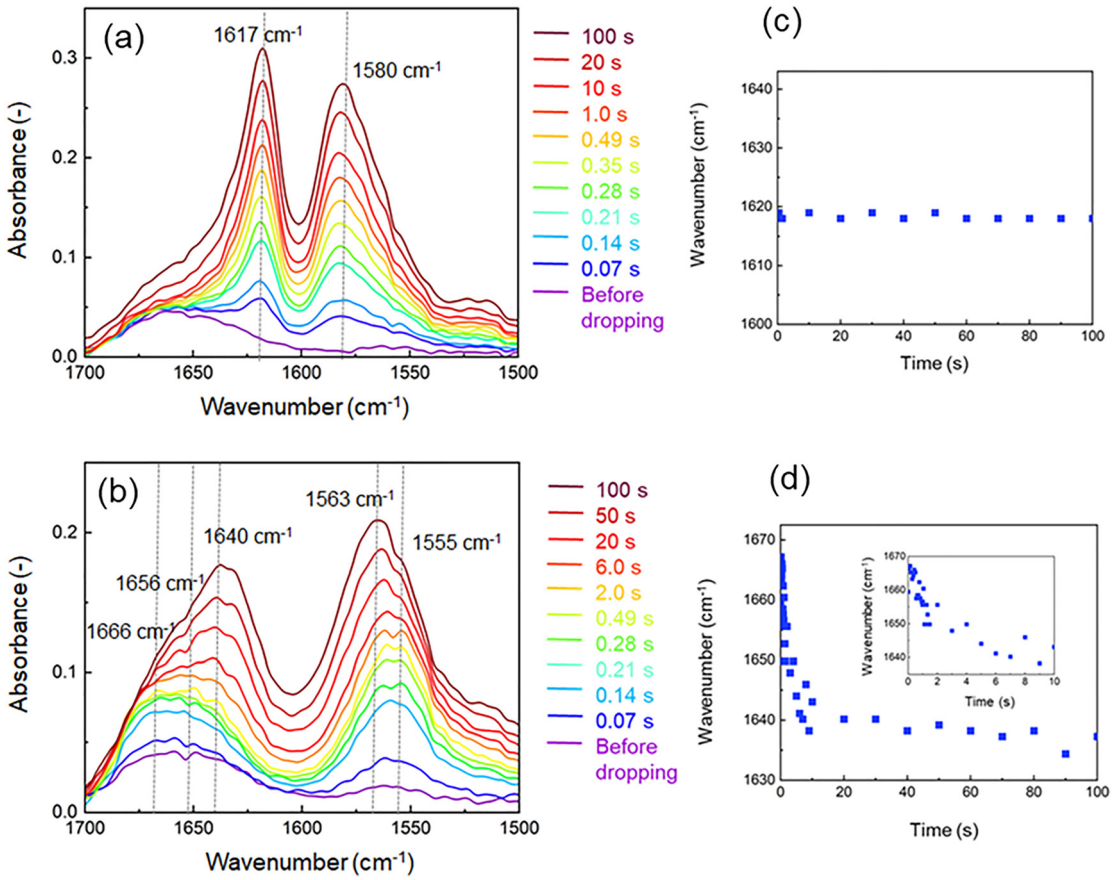

Fig. 7 ATR spectra as a function of time in the 0–100 s range for the polyaddition reactions (a) between hexamethylenediamine (HDA)/dimethyl sulfoxide (DMSO) and hexamethylene diisocyanate (HDI)/DMSO and (b) between 1,3-bis(aminomethyl)cyclohexane (H6XDA)/DMSO and 1,3-bis(isocyanatomethyl)cyclohexane (H6XDI)/DMSO. Shifts in the ν(C═O) IR peak during the reactions (c) between HDI/DMSO and HDA/DMSO and (d) between H6XDI/DMSO and H6XDA/DMSO (the inset shows the first 10 s).

1666 cm^{-1} in the initial 0.5 s of the reaction between H6XDI and H6XDA, which suggests that the hydrogen bonds formed were mainly disordered. The peak position shifted to 1656 cm^{-1} beyond the 0.5–2 s range, which indicates that the hydrogen bonds remained disordered but were stronger than those formed in the first 0.5 s. The ν(C═O) peak subsequently shifted to 1640 cm^{-1} as the reaction progressed, indicative of the formation of ordered hydrogen bonds. Hence, the urea groups formed stronger ordered hydrogen bonds over time during the polyaddition reaction of alicyclic H6XDI and H6XDA, although poor hydrogen bonding was observed in the initial stage of the reaction. However, in the case of alicyclic H6XDI and H6XDA, the half bandwidth of the ν(C═O) and δ(N–H) bands is wider compared to the case of aliphatic HDI and HDA. In addition, the intensity ratio of the ν(C═O) and $\delta(NH_2)$ absorption bands differed between the alicyclic and aliphatic cases. These results suggest that the hydrogen bonding order of polyurea formed from H6XDI and H6XDA was lower than that formed from HDI and HDA.

The schematic diagram in Fig. 8 shows the formation of polyurea and intermolecular hydrogen bonds. The aliphatic HDA and HDI monomers are linear molecules with methylene groups; consequently, the polyaddition product experiences little steric hindrance near the urea groups, leading to short inter-urea distances. Therefore, ordered hydrogen bonds easily form concurrently with polyurea formation. In contrast, the polyurea formed from H6XDA and H6XDI experiences steric hindrance near the urea groups; consequently, hydrogen bonds form with difficulty, and poor hydrogen bonding is observed in the initial stage of polyurea formation. However, inter-urea distances decrease as the reaction progresses owing to polyurea aggregation, which would enhance hydrogen bonding and lead to an ordered state. However, poorly ordered hydrogen bonds remained in the polyurea. These results reveal that intermolecular hydrogen bonding during polyurea formation depends on the monomer structure.

Experimental

Materials

The aliphatic monomers HDA and HDI and the DMSO solvent were purchased from Nacalai Tesque (Japan). The alicyclic monomers H6XDA and H6XDI were purchased from Tokyo Chemical Industry (Tokyo, Japan).

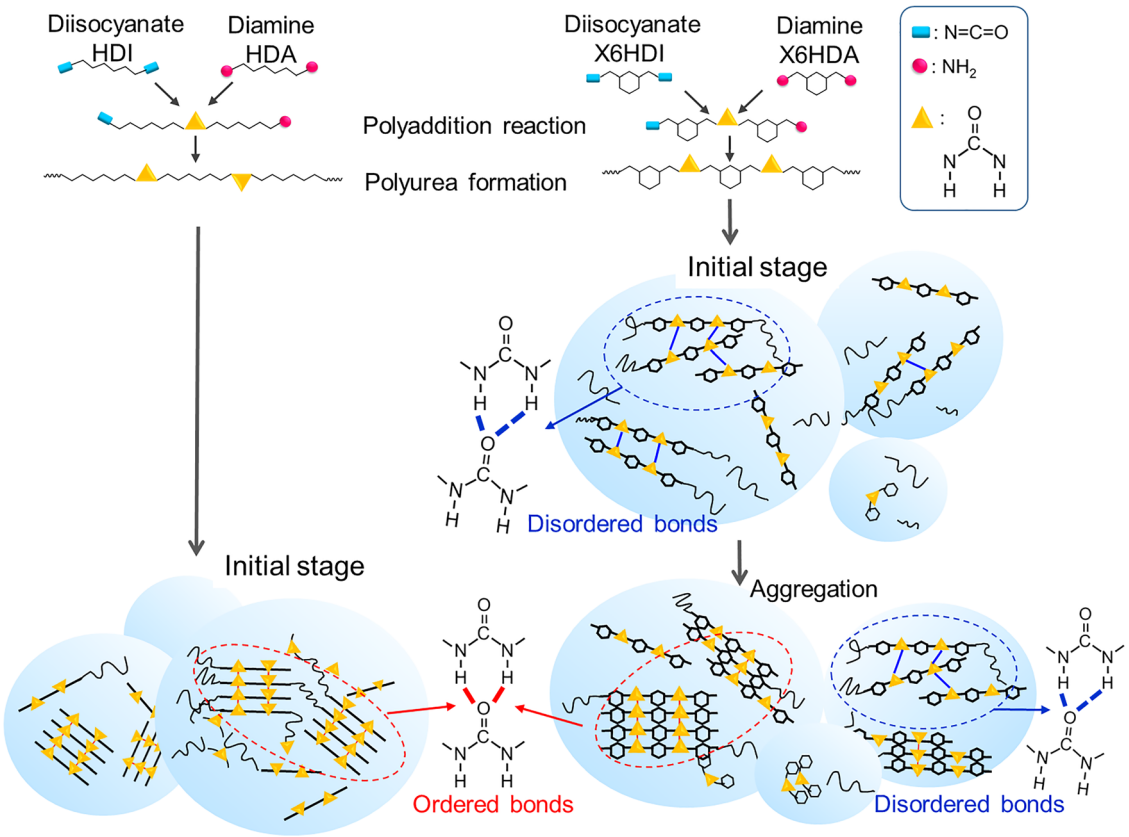

Fig. 8 Schematic of the polyaddition reactions of aliphatic and alicyclic diamines and diisocyanates and formation of intermolecular hydrogen bonds in polyurea.

Observation of polyurea formation by time-resolved FTIR-ATR spectroscopy

HDA, HDI, H6XDA, and H6XDI were dissolved in DMSO, each at a concentration of 1.0 M. FTIR spectroscopy was performed using an FT/IR-6600 FTIR spectrometer (Jasco) equipped with an ATR PRO ONE single-reflection ATR unit (Jasco) with a diamond prism. The ATR measurement was performed under non-polarized conditions. Fast time-resolved FTIR spectra were rapidly acquired using a mercury–cadmium–telluride detector, with spectral acquisition intervals that varied with resolution. The resolution was 4 cm^{-1} in this experiment; hence, spectra were acquired at intervals of approximately 70 ms for 5 min. The diisocyanate solution (0.1 μL) was dropped onto the ATR prism under flowing nitrogen prior to the experiment, and the diamine solution (0.1 μL) was added immediately after ATR spectral acquisition had commenced. The ATR phenomenon differs from that of absorption of IR, used in measurement of typical transmission or absorption spectra.[35,36] In ATR-FT-IR, the attenuation of IR can be considered due to absorption. Because the attenuation of IR is dependent on IR wavelength, the ATR spectrum differs from the conventional FT-IR spectrum. However, we used ATR spectra without correction in our experiment.

Conclusions

In this study, we focused on the very fast formation reaction of polyurea, whose intramolecular polarization is derived from the urea group, has excellent mechanical properties owing to intermolecular hydrogen bonding, and has recently been the subject of research as a material for 3D printers. We aimed to observe and analyze polyurea formation *via* the polyaddition of a diamine to a diisocyanate, which proceeds within seconds, by *in situ* rapid-scan FTIR spectroscopy. Variations in the absorption spectrum over the first 1 s of the reaction were analyzed using chemical kinetics. The polyaddition reactions of aliphatic and alicyclic diamine and diisocyanate monomers were analyzed using a second-order reaction model. Reaction rate constants of 7.75 and 8.21 L mol^{-1} s^{-1} were obtained for the reactions between HDI/DMSO and HAD/DMSO and between H6XDI/DMSO and H6XAD/DMSO, respectively. Additionally, we focused on the relationship between polyurea formation and changes in intermolecular hydrogen bonding states. The formation of polyurea and its intermolecular hydrogen bonds were investigated based on the shift in the position of the ν(C═O) peak derived from the urea group of the generated polyurea. Strong hydrogen bonding was observed in the initial stage of aliphatic polyurea formation. On the other hand, alicyclic polyurea exhibited weak hydrogen bonding in the initial stage of formation (approximately 10 s), which strengthened over time. The difference in intermolecular hydrogen bonding during polyurea formation was attributed to the difference in the monomer structure. We were able to clarify the changes in intermolecular hydrogen bonding states during polyurea formation, which occur within tens of seconds, according to the

monomer structure. This study demonstrates that rapid-scan time-resolved FTIR spectroscopy is a powerful tool for analyzing the fast reactions involved in polyurea formation, which had previously been difficult to characterize. We believe that this technique can also be used to observe other fast reactions, such as the curing reaction of materials in 3D printer inks. Furthermore, clarifying the effects of the diamine and diisocyanate structures on polyurea formation and hydrogen bonding states will be useful for future polyurea research, which is expected to have a variety of applications.

Author contributions

K. I. and Y. K. designed and conceived the study. Y. K. and S. A. drafted the manuscript under the supervision and guidance of S. H., T. F., and K. I. S. A. and Y. K. performed the measurements and analyzed the experimental data. The manuscript was written with contributions from all authors. All authors approved the final version of the manuscript.

Conflicts of interest

There are no conflicts to declare.

Data availability

The data supporting the findings of this study are available within the paper and its supplementary information (SI). Supplementary information is available. See DOI: **https://doi.org/10.1039/d5cp02518d**.

Acknowledgements

This work was partially supported by JSPS KAKENHI (grant numbers 21H04655 and 24H00422).

References

1 X. Ou, X. Zou, Q. Liu, L. Li, S. Li, Y. Cui, Y. Zhou and F. Yan, *Chem. Mater.*, 2023, **35**, 1218–1228.
2 T. Li, C. Zhang, Z. Xie, J. Xu and B.-H. Guo, *Polymer*, 2018, **145**, 261–271.
3 A. M. Castagna, A. Pangon, G. P. Dillon and J. Runt, *Macromolecules*, 2013, **46**, 6520–6527.
4 M. Morimoto, T. Fukutomi, Y. Koshiba and K. Ishida, *J. Mater. Sci.*, 2019, **54**, 2483–2492.
5 D. Fragiadakis, R. Gamache, R. B. Bogoslovov and C. M. Roland, *Polymer*, 2010, **51**, 178–184.
6 M. Grujicic, T. He, B. Pandurangan, F. R. Svingala, G. S. Settles and M. J. Hargather, *J. Mater. Eng. Perform.*, 2012, **21**, 2–16.
7 L. Lu, J. Xu, J. Li, Y. Xing, Z. Zhou and F. Zhang, *Macromolecules*, 2024, **57**, 2100–2109.
8 D. S. Bergsman, R. G. Closser, C. J. Tassone, B. M. Clemens, D. Nordlund and S. F. Bent, *Chem. Mater.*, 2017, **29**, 1192–1203.
9 G. Toader, E. Rusen, M. Teodorescu, A. Diacon, P. O. Stanescu, T. Rotariu and A. Rotariu, *J. Appl. Polym. Sci.*, 2016, **133**, 43967.
10 A. M. Castagna, A. Pangon, T. Choi, G. P. Dillon and J. Runt, *Macromolecules*, 2012, **45**, 8438–8444.
11 T. Choi, D. Fragiadakis, C. M. Roland and J. Runt, *Macromolecules*, 2012, **45**, 3581–3589.
12 Y. Taguchi, M. Furukawa and T. Yokoyama, *Nippon Gomu Kyokaishi*, 1993, **66**, 253–258.
13 Z. Zhang, L. Qian, J. Cheng, Q. Xie, C. Ma and G. Zhang, *Chem. Mater.*, 2023, **35**, 1806–1817.
14 T. Tanaka, A. Tsuji, A. Shimoyama, M. Hayakawa, R. Matsubara and A. Kubono, *Jpn. J. Appl. Phys.*, 2020, **59**, 036502.
15 M. Morimoto, Y. Koshiba, M. Misaki and K. Ishida, *Appl. Phys. Express*, 2015, **8**, 101501.
16 Z. Zhao, Y. Feng, L. Yang, S. Zhang, X. Liu, Y. Zhang, M. Li and S. Li, *Appl. Phys. Lett.*, 2023, **123**, 232901.
17 B. Shojaei, M. Najafi, A. Yazdanbakhsh, M. Abtahi and C. Zhang, *Polym. Adv. Technol.*, 2021, **32**, 2797–2812.
18 V. Shahi, V. Alizadeh and A. V. Amirkhizi, *Mech. Time Depend. Mater.*, 2021, **25**, 447–471.
19 M. Tripathi, S. Parthasarathy and P. K. Roy, *J. Appl. Polym. Sci.*, 2020, **137**, 7373.
20 J. L. Stanford, R. H. Still and N. A. Wilkinson, *Polymer*, 1995, **36**, 3555–3564.
21 X. Chen, C. E. Zawaski, G. A. Spiering, B. Liu, C. M. Orsino, R. B. Moore, C. B. Williams and T. E. Long, *ACS Appl. Mater. Interfaces*, 2020, **12**, 32006–32016.
22 M. Zawadzki, K. Zawada, S. Kowalczyk, A. Plichta, J. Jaczewski and T. Zabielskic, *RSC Adv.*, 2022, **12**, 3406–3415.
23 W. Song and J. Liu, *J. Appl. Polym. Sci.*, 2012, **123**, 479–484.
24 K. Sahre, M. H. Abd Elrehim, K.-J. Eichhorn and B. Voit, *Macromol. Mater. Eng.*, 2006, **291**, 470–476.
25 P. Schuchardt and H. W. Siesler, *Anal. Bioanal. Chem.*, 2017, **409**, 833–839.
26 C. S. Paik Sung, T. W. Smith and N. H. Sung, *Macromolecules*, 1980, **13**, 117–121.
27 M. M. Coleman, K. H. Lee, D. J. Skrovanek and P. C. Painter, *Macromolecules*, 1986, **19**, 2149–2157.
28 M. M. Coleman, M. Sobkowiak, G. J. Pehlert, P. C. Painter and T. Iqbal, *Macromol. Chem. Phys.*, 1997, **198**, 117–136.
29 J. Mattia and P. Painter, *Macromolecules*, 2007, **40**, 1546–1554.
30 N. Iqbal, M. Tripathi, S. Parthasarathy, D. Kumar and P. K. Roy, *ChemistrySelect*, 2018, **3**, 1976–1982.
31 K. Chen, J. Yu, G. Guzman, S. S. Es-haghi, M. L. Becker and M. Cakmak, *Macromolecules*, 2017, **50**, 1075–1084.
32 T. Yuzawa, C. Kato, M. W. George and H. O. Hamaguchi, *Appl. Spectrosc.*, 1994, **48**, 684–690.
33 O. Weidlich and F. Siebert, *Appl. Spectrosc.*, 1993, **47**, 1394–1400.
34 P. W. Loscutoff, H. Zhou, S. B. Clendenning and S. F. Bent, *ACS Nano*, 2010, **4**, 331–341.
35 A. L. Averett, R. P. Griffiths and K. Nishikida, Effective Path Length in Attenuated Total Reflection Spectroscopy, *Anal. Chem.*, 2008, **80**, 3045–3049.
36 S. Vahur, A. Teearu, P. Peets, L. Joosu and I. Leito, ATR-FT-IR spectral collection of conservation materials in the extended region of 4000–80 cm^{-1}, *Anal. Bioanal. Chem.*, 2016, **408**, 3373–3379.